

## Electronic Supplementary Information (ESI)

# Luminescent Eu<sup>III</sup> and Tb<sup>III</sup> bimetallic complexes of *N, N'*-heterocyclic bases and tolfenamic acid: structures, photophysical Aspects and biological activity

Zafar Abbas,<sup>a</sup> Prerana Singh,<sup>b,c</sup> Srikanth Dasari,<sup>a</sup> Sri Sivakumar,<sup>b,d</sup> Ashis K. Patra,<sup>\*,a</sup>

<sup>a</sup> Department of Chemistry, Indian Institute of Technology Kanpur, Kanpur 208016, Uttar Pradesh, India

<sup>b</sup> Department of Chemical Engineering and Centre for Nanosciences, Indian Institute of Technology Kanpur, Kanpur 208016, Uttar Pradesh, India

<sup>c</sup> Department of Biological Sciences and Bioengineering, Indian Institute of Technology Kanpur, Kanpur 208016, Kanpur, India

<sup>d</sup> Centre for Environmental Science & Engineering, Indian Institute of Technology Kanpur, Kanpur, 208016, India

Table of Contents	Page No.
<b>Figure S1:</b> Overlay of FT-IR spectra of the complexes <b>1-4</b> .	S3
<b>Figure S2:</b> Time dependent UV-Vis absorption spectral of complex <b>1-4</b> recorded for 4 h at an interval of 10 min.	S4
<b>Figure S3:</b> The Ln <sup>III</sup> -Ln <sup>III</sup> bond lengths (Å) in the structure of the complexes <b>1-4</b> .	S5
<b>Figure S4:</b> The Ln <sup>III</sup> -O donor bond lengths (Å) of the chelating TFA ligand in the structure of the complexes <b>1-4</b> .	S6
<b>Figure S5:</b> The Ln <sup>III</sup> -O donor bond lengths (Å) of the bridging TFA ligand in the structure of the complexes <b>1-4</b> .	S7
<b>Figure S6:</b> The Ln <sup>III</sup> -N donor bond lengths (Å) in the structure of the complexes <b>1-4</b> .	S8
<b>Figure S7:</b> Pi-Pi stacking distances (Å) between DPQ/DPPZ in lattice of the complexes <b>1 &amp; 2</b> .	S9
<b>Figure S8:</b> Pi-Pi stacking distances (Å) between DPQ/DPPZ in lattice of the complexes <b>3 &amp; 4</b> .	S10
<b>Figure S9:</b> Absorption spectral titration of complex <b>2-4</b> with increasing concentration of CT-DNA.	S11
<b>Figure S10:</b> Quenching of emission intensity of EB-DNA adduct using EB displacement assay study with the addition of complex <b>2-4</b> .	S12
<b>Figure S11:</b> Emission spectral titration of BSA (5 μM) with complex <b>1-4</b> showing quenching in the emission of tryptophan residue.	S13
<b>Figure S12:</b> Synchronous emission spectra of BSA with increasing concentration of complex <b>1</b> with Δλ=15 nm ( <b>a</b> ) and Δλ=60 nm ( <b>b</b> ).	S14
<b>Figure S13:</b> Synchronous emission spectra of BSA with increasing concentration of complex <b>2</b> with Δλ=15 nm ( <b>a</b> ) and Δλ=60 nm ( <b>b</b> ).	S14
<b>Figure S14:</b> Synchronous emission spectra of BSA with increasing concentration of complex <b>3</b> with Δλ=15 nm ( <b>a</b> ) and Δλ=60 nm ( <b>b</b> ).	S15
<b>Figure S15:</b> Synchronous emission spectra of BSA with increasing concentration of complex <b>4</b> with Δλ=15 nm ( <b>a</b> ) and Δλ=60 nm ( <b>b</b> ).	S15
<b>Figure S16:</b> Cytotoxicity profile of complex <b>1</b> in HeLa and MCF-7 Cell lines.	S16
<b>Figure S17:</b> Cytotoxicity profile of complex <b>2</b> in HeLa and MCF-7 Cell lines.	S16
<b>Figure S18:</b> Cytotoxicity profile of complex <b>3</b> in HeLa and MCF-7 Cell lines.	S17
<b>Figure S19:</b> Cytotoxicity profile of complex <b>4</b> in HeLa and MCF-7 Cell lines.	S17
<b>Figure S20:</b> Photoinduced cytotoxicity profile of complex <b>1</b> by exposure to UV-A light in MCF-7 cell line.	S18
<b>Figure S21:</b> Photoinduced cytotoxicity profile of complex <b>3</b> by exposure to UV-A light in MCF-7 cell line.	S18
<b>Figure S22:</b> Confocal laser scanning microscopy images (CLSM) of cellular localization in the HeLa and MCF-7 cell lines treated with complex <b>1</b> .	S19
<b>Figure S23:</b> Confocal laser scanning microscopy images (CLSM) of cellular localization in the HeLa and MCF-7 cell lines treated with complex <b>4</b> .	S20
<b>Experimental Section:</b> Materials and methods.	S21

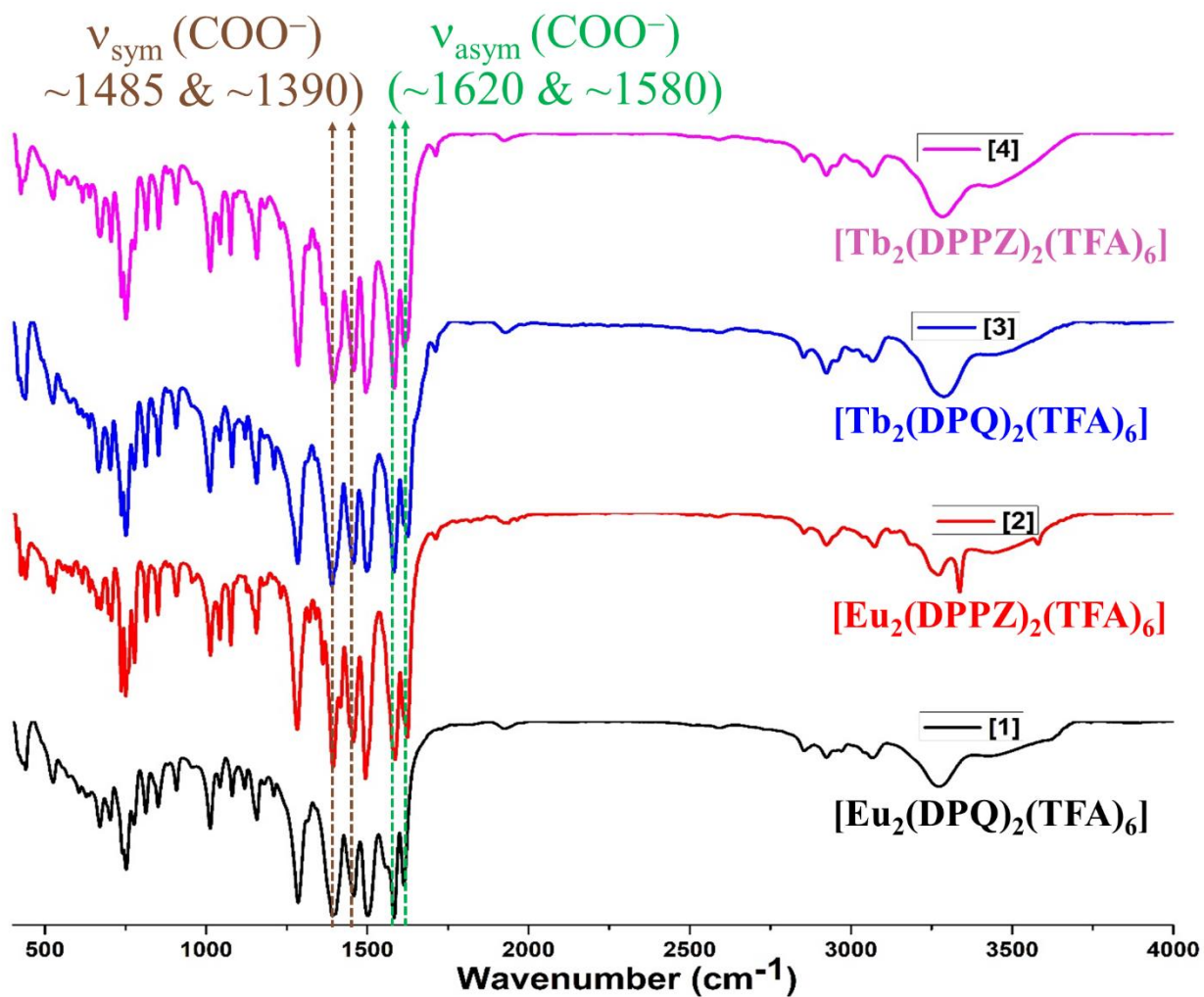


**Figure S1:** FT-IR spectra of the complexes **1-4** recorded using KBr disc in the range 400-4000  $\text{cm}^{-1}$  shows the isostructural behavior of the complexes in solid state observed from close resemblances in the finger-print region.

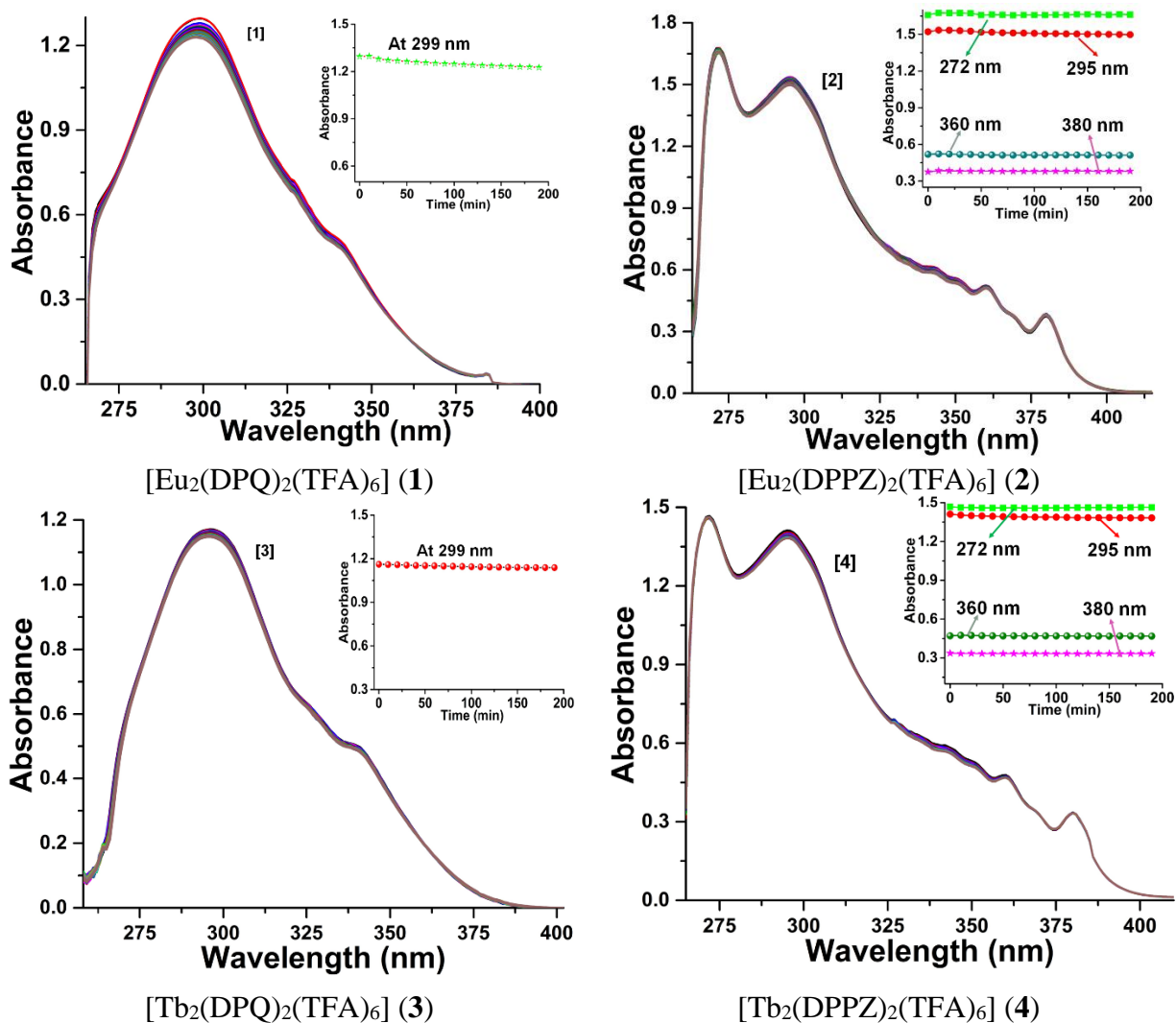


**Figure S2:** UV-Vis absorption spectra of the complexes **1-4** ( $10 \mu\text{M}$ ) in acetonitrile/DMF (95/5) for a period of 4 h at a time interval of 10 min at 298 K. Inset shows variation in the absorbance of complexes at 272, 295, 299, 360 and 380 nm with time.

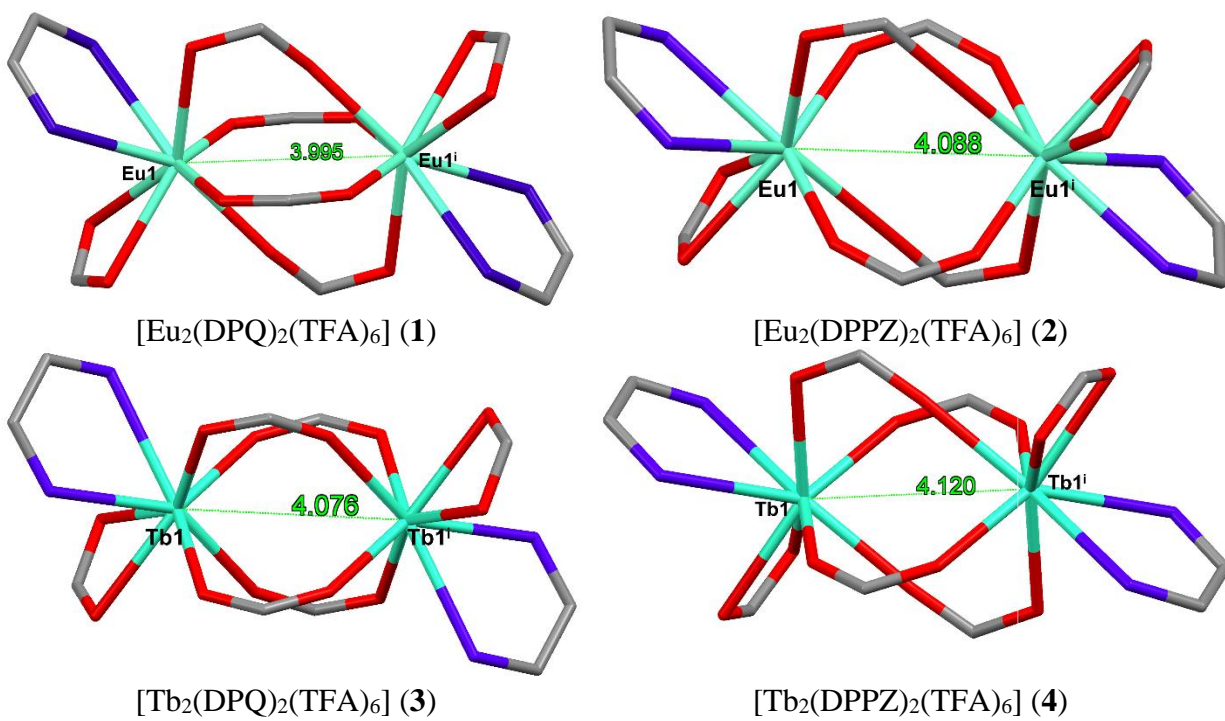
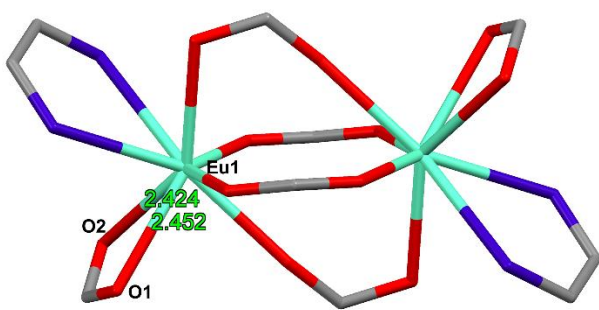
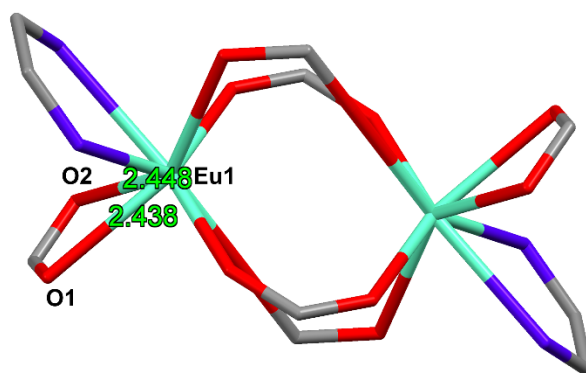


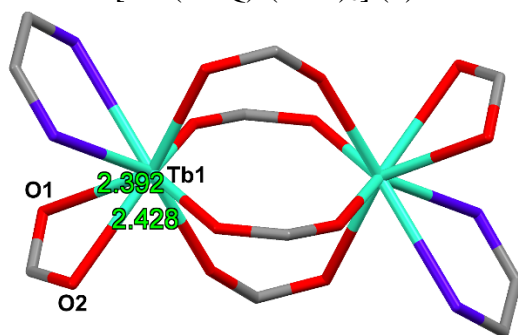
**Figure S3:** The Ln<sup>III</sup>-Ln<sup>III</sup> bond lengths (Å) in the structure of the complexes 1-4.



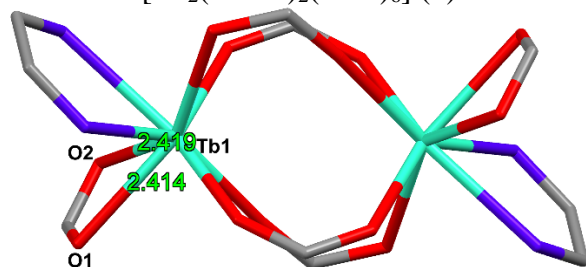
[Eu<sub>2</sub>(DPQ)<sub>2</sub>(TFA)<sub>6</sub>] (1)



[Eu<sub>2</sub>(DPPZ)<sub>2</sub>(TFA)<sub>6</sub>] (2)

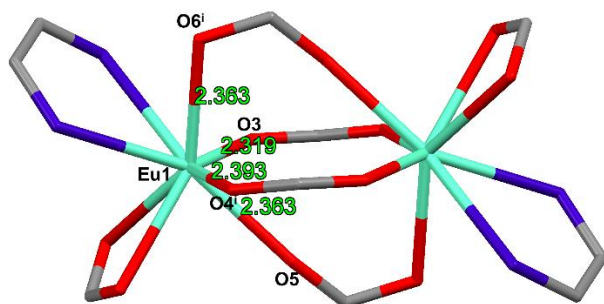


[Tb<sub>2</sub>(DPQ)<sub>2</sub>(TFA)<sub>6</sub>] (3)

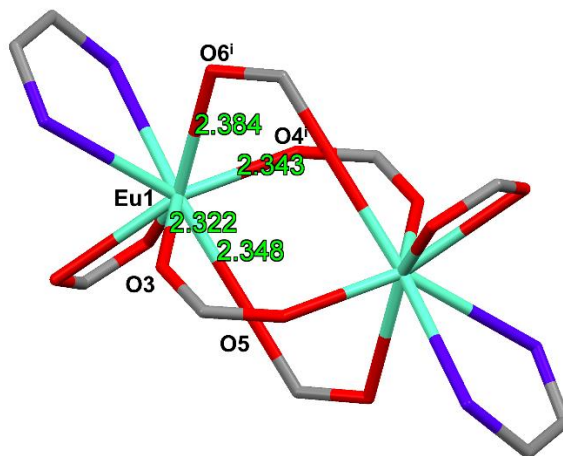


[Tb<sub>2</sub>(DPPZ)<sub>2</sub>(TFA)<sub>6</sub>] (4)

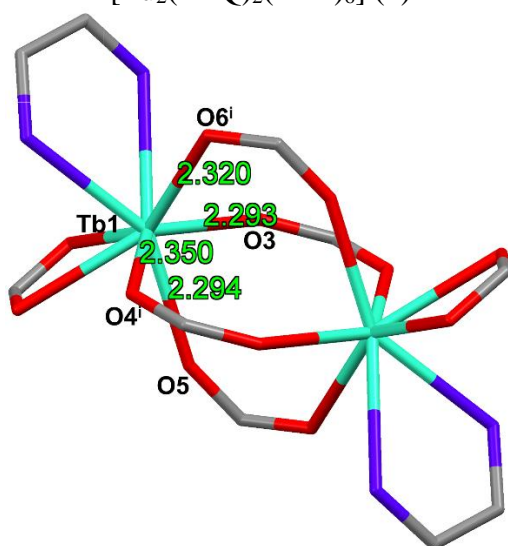
**Figure S4:** The Ln<sup>III</sup>-O donor bond lengths (Å) of the chelating TFA ligand in the structure of the complexes 1-4.



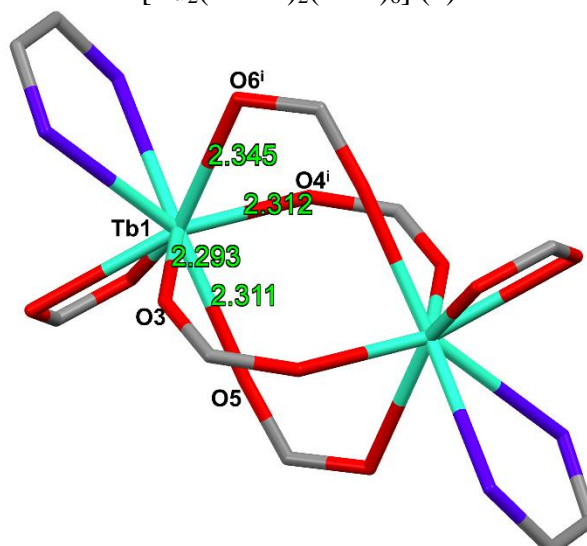
[Eu<sub>2</sub>(DPQ)<sub>2</sub>(TFA)<sub>6</sub>] (1)



[Eu<sub>2</sub>(DPPZ)<sub>2</sub>(TFA)<sub>6</sub>] (2)

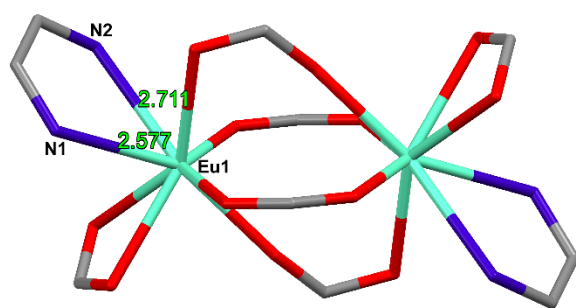


[Tb<sub>2</sub>(DPQ)<sub>2</sub>(TFA)<sub>6</sub>] (3)

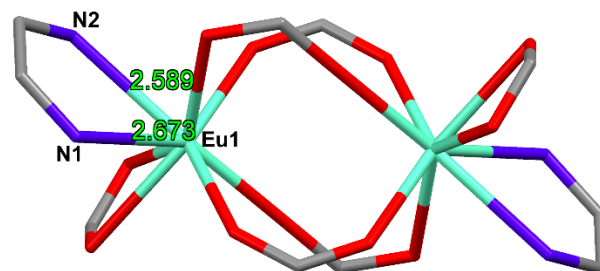


[Tb<sub>2</sub>(DPPZ)<sub>2</sub>(TFA)<sub>6</sub>] (4)

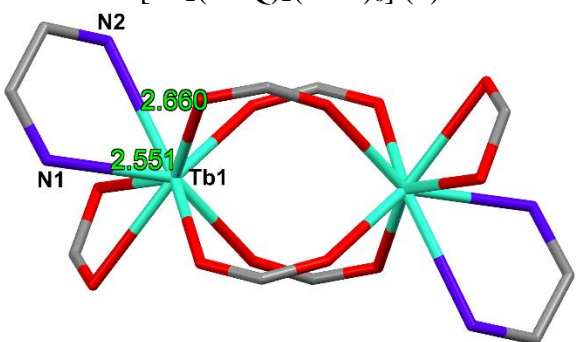
**Figure S5:** The Ln<sup>III</sup>-O donor bond lengths (Å) of the bridging TFA ligand in the structure of the complexes 1-4.



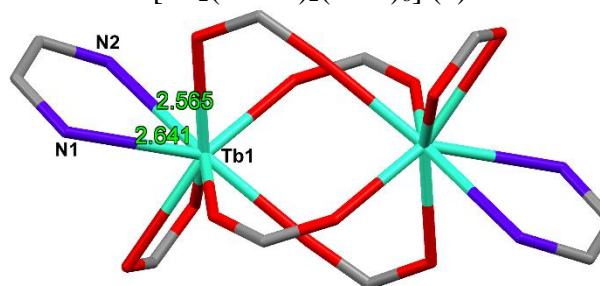
[Eu<sub>2</sub>(DPQ)<sub>2</sub>(TFA)<sub>6</sub>] (1)



[Eu<sub>2</sub>(DPPZ)<sub>2</sub>(TFA)<sub>6</sub>] (2)

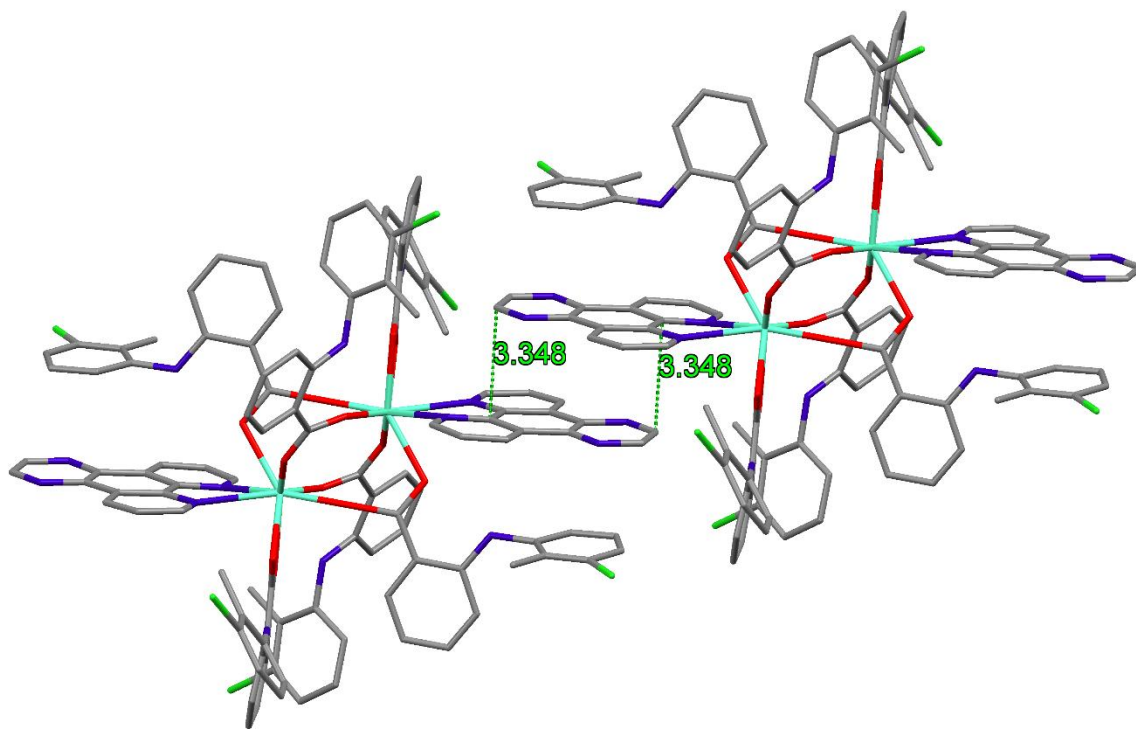


[Tb<sub>2</sub>(DPQ)<sub>2</sub>(TFA)<sub>6</sub>] (3)

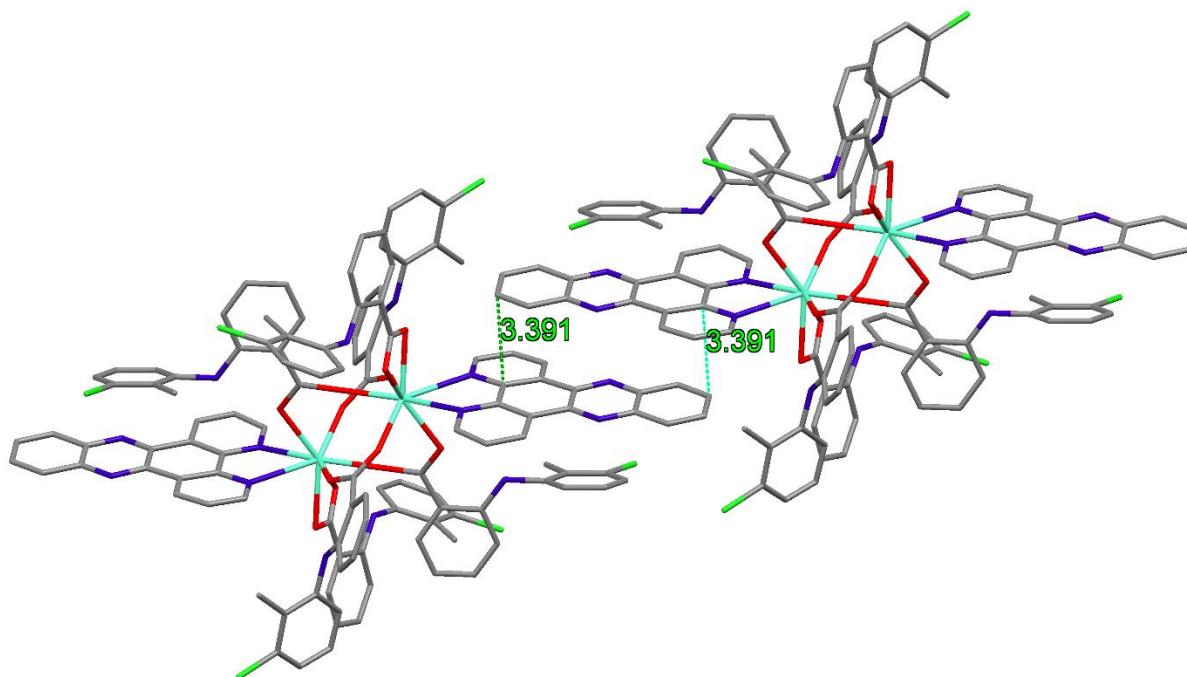


[Tb<sub>2</sub>(DPPZ)<sub>2</sub>(TFA)<sub>6</sub>] (4)

**Figure S6:** The Ln<sup>III</sup>-N donor bond lengths (Å) in the structure of the complexes 1-4.

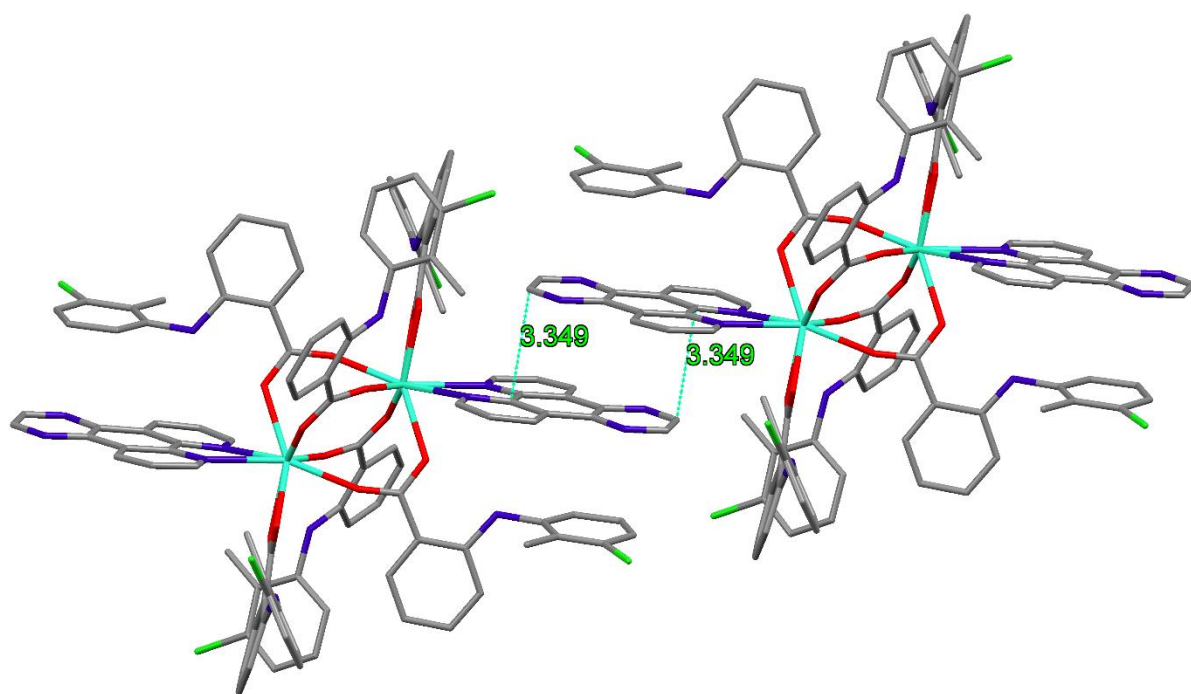


$[\text{Eu}_2(\text{DPQ})_2(\text{TFA})_6]$  (1)

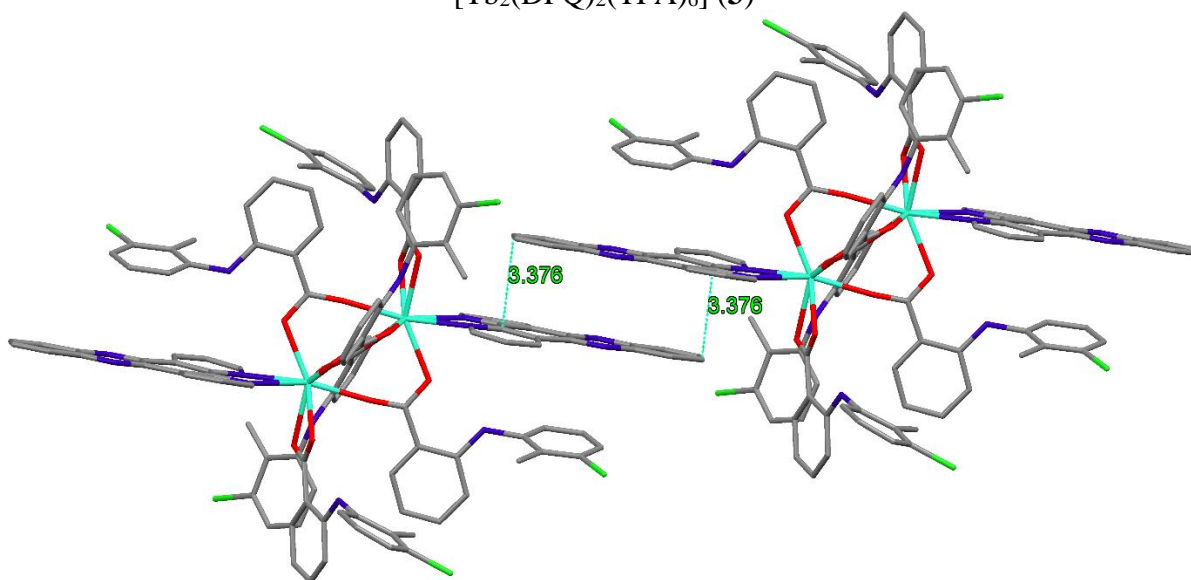


$[\text{Eu}_2(\text{DPPZ})_2(\text{TFA})_6]$  (2)

**Figure S7:** Pi-Pi stacking distances (Å) between DPQ/DPPZ in lattice of the complexes **1** (top) & **2** (bottom).



$[\text{Tb}_2(\text{DPQ})_2(\text{TFA})_6]$  (3)



$[\text{Tb}_2(\text{DPPZ})_2(\text{TFA})_6]$  (4)

**Figure S8:** Pi-Pi stacking distances (Å) between DPQ/DPPZ in lattice of the complexes 3 & 4 (Up and Down).

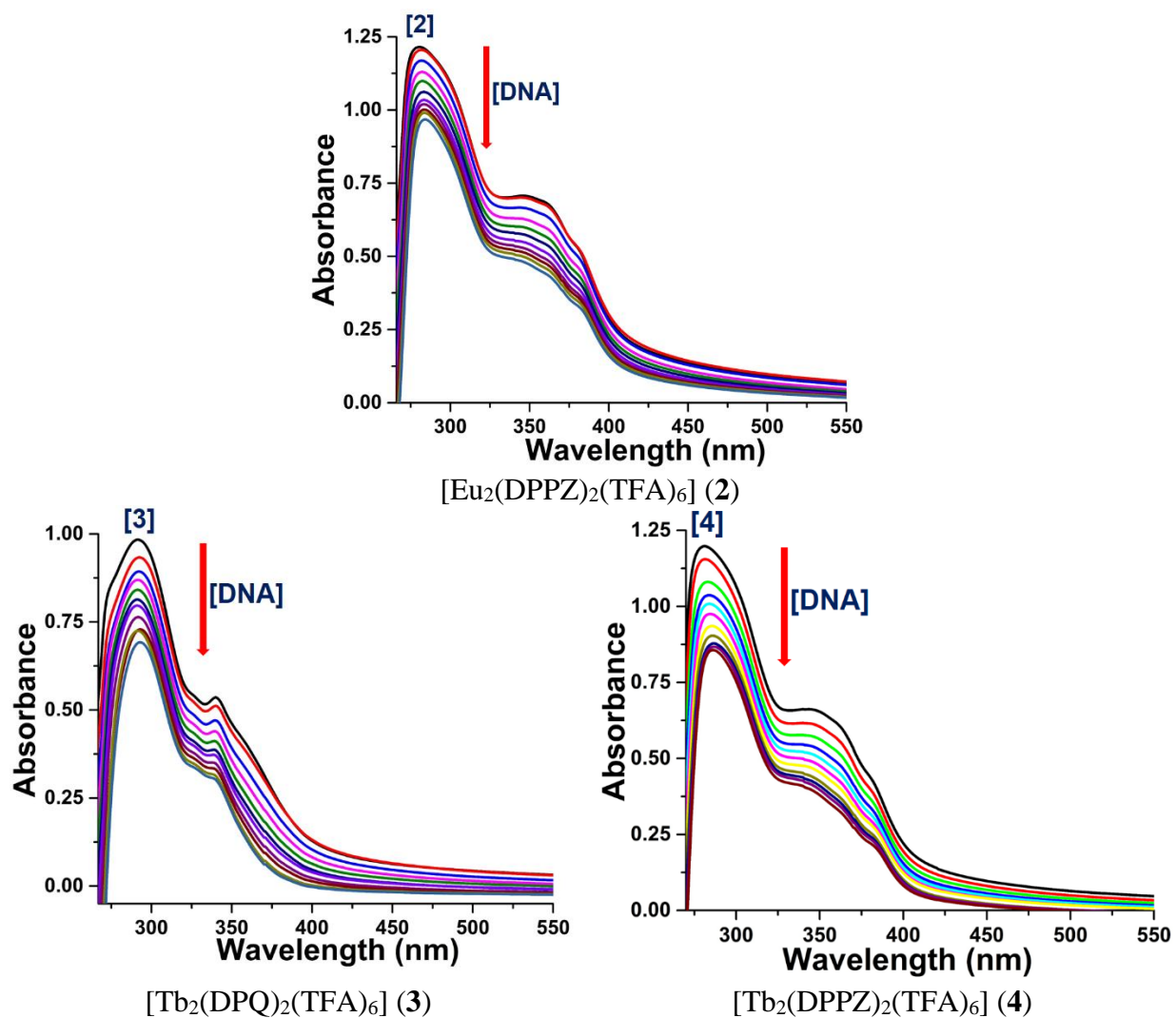


**Figure S9:** Absorption spectral titration of complexes (2-4) ( $10 \mu\text{M}$ ) with increasing concentration of CT-DNA in 5 mM Tris HCl-NaCl buffer (pH = 7.2) showing the hypochromic shift in absorbance band. Arrow decrease in intensity of absorption band with increasing DNA concentration.

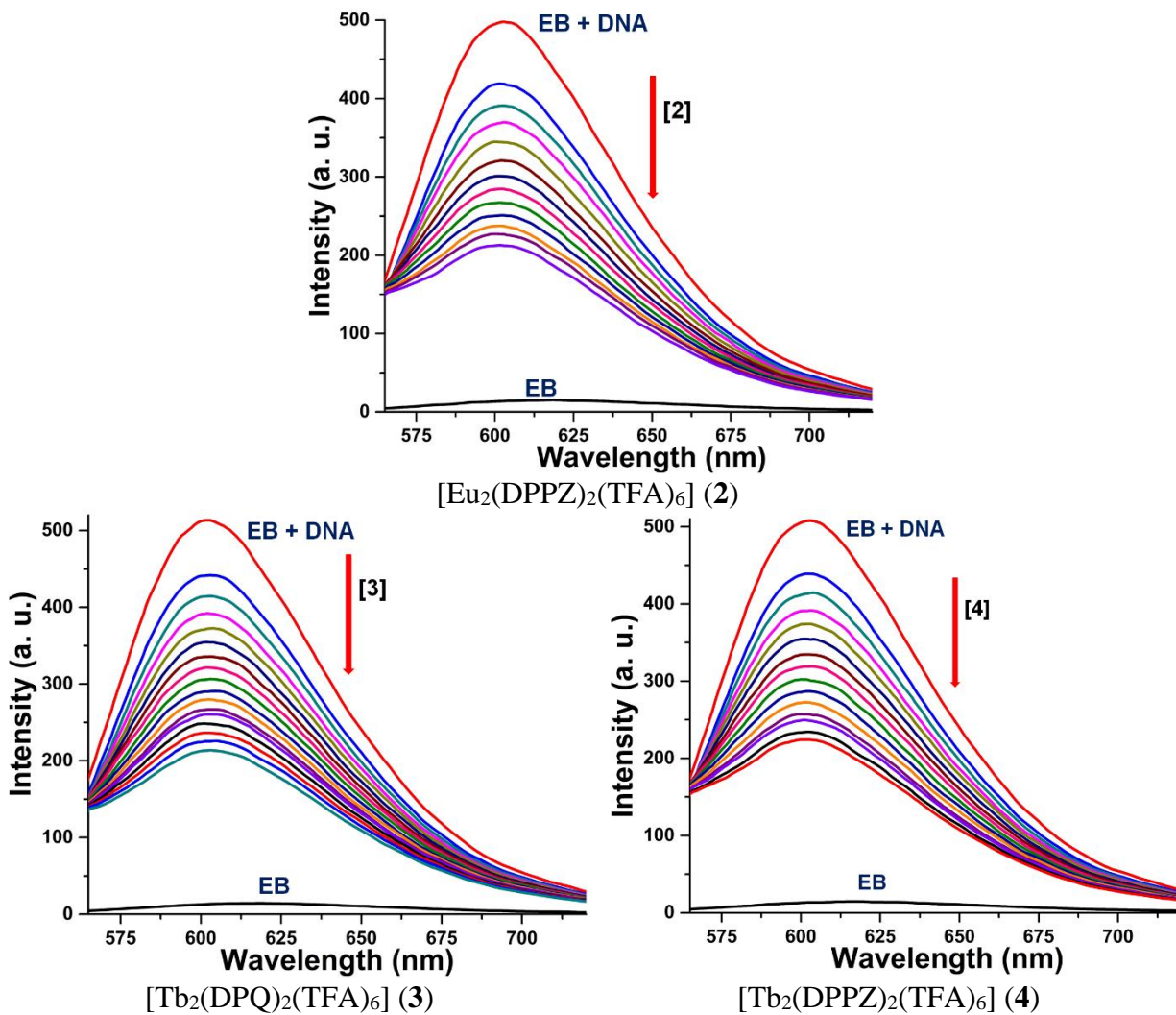


**Figure S10:** Quenching of emission intensity of EB-DNA adduct at 603 nm ( $\lambda_{ex} = 546$  nm) with the addition of complexes (2-4) in 5 mM Tris-HCl/5 mM NaCl buffer (pH = 7.2) at 298 K. arrows shows the increase in concentration of the complexes displaces EB from its adduct EB-DNA causing quenching in emission. Slit width (Excitation and Emission) = 5 nm, [EB] = 12  $\mu$ M.

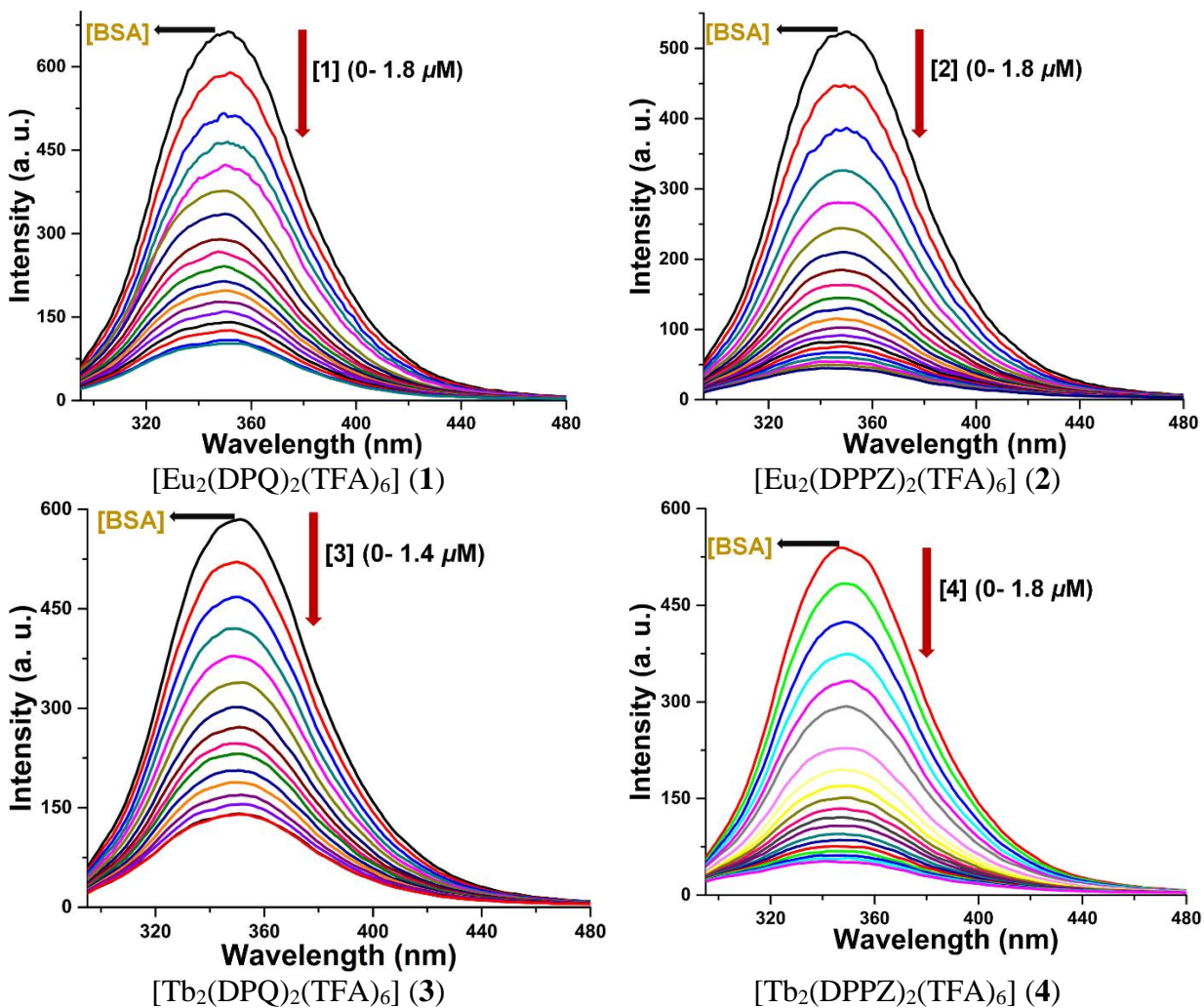


**Figure S11:** Emission spectral titration of BSA (5  $\mu\text{M}$ ) with complexes (1-4) in 5 mM Tris HCl-NaCl buffer (pH = 7.2) showing quenching in the emission (350 nm) of tryptophan residue at 280 nm excitation. Upside down arrow (red) shows hypochromic shift in the intensity of emission with increasing concentration of complex. Slit width (Excitation and Emission) = 5 nm.

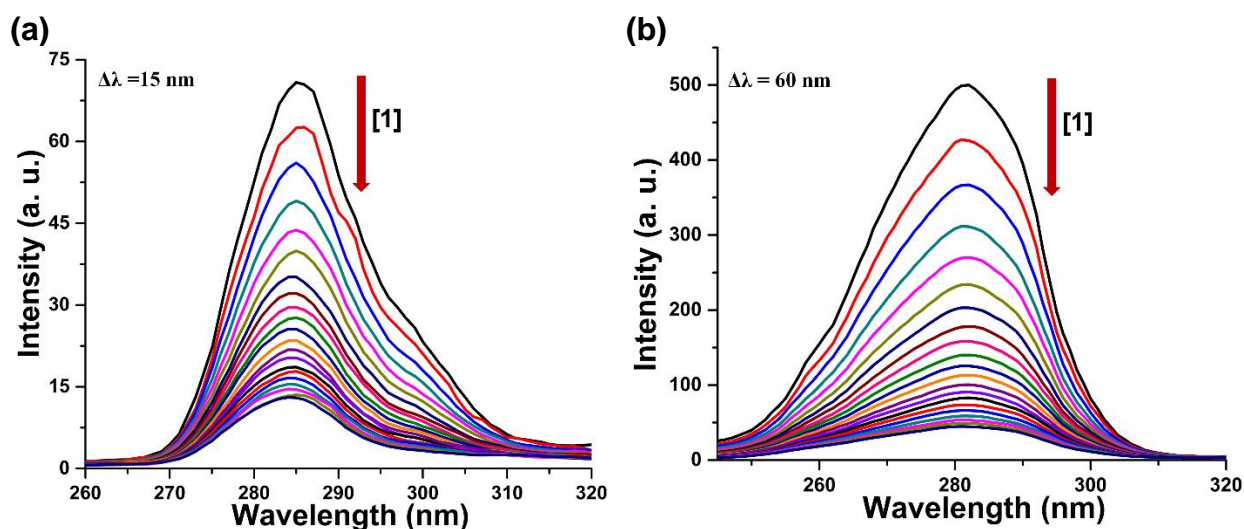


**Figure S12:** Synchronous emission spectra measurement of BSA ( $5 \mu\text{M}$ ) with increasing concentration of  $[\text{Eu}_2(\text{DPQ})_2(\text{TFA})_6]$  (**1**) with  $\Delta\lambda=15 \text{ nm}$  (**a**) and  $\Delta\lambda=60 \text{ nm}$  (**b**) in 5 mM Tris-HCl 5 mM NaCl buffer (pH = 7.2) at 298 K. Arrow shows the quenching in the emission of BSA with addition of complex. Slit width (Excitation and Emission) = 5 nm.

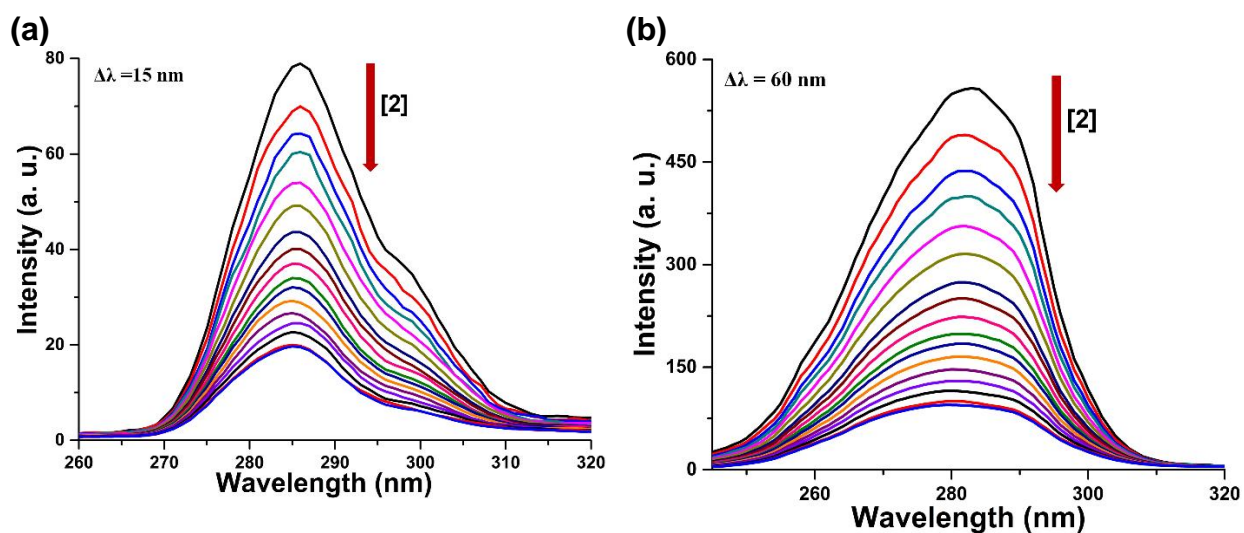


**Figure S13:** Synchronous emission spectra measurement of BSA ( $5 \mu\text{M}$ ) with increasing concentration of  $[\text{Eu}_2(\text{DPPZ})_2(\text{TFA})_6]$  (**2**) with  $\Delta\lambda=15 \text{ nm}$  (**a**) and  $\Delta\lambda=60 \text{ nm}$  (**b**) in 5mM Tris-HCl/5mM NaCl buffer (pH = 7.2) at 298 K. Arrow shows the quenching in the emission of BSA with addition of complex. Slit width (Excitation and Emission) = 5 nm.

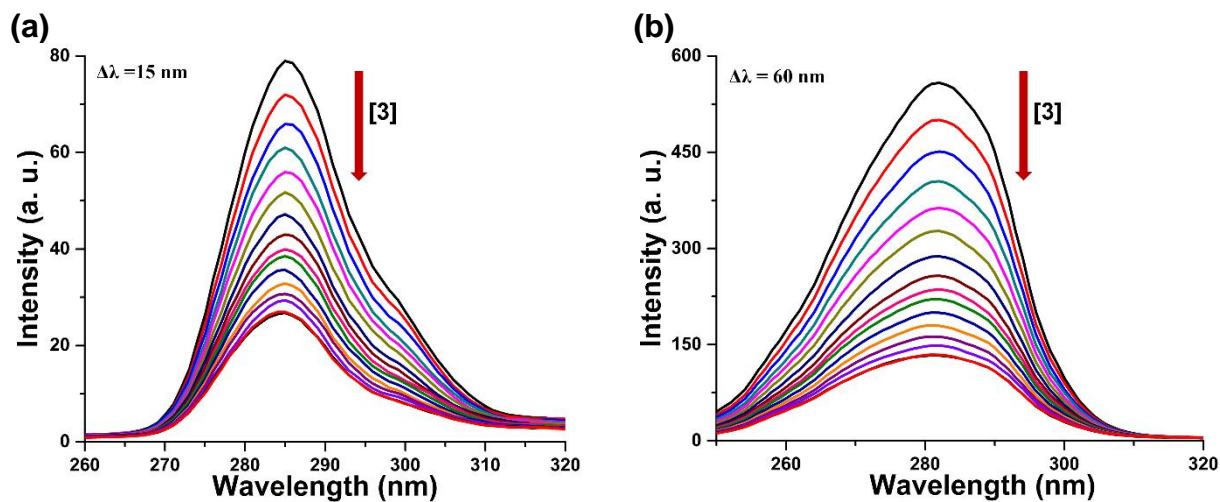


**Figure S14:** Synchronous emission spectra measurement of BSA ( $5 \mu\text{M}$ ) with increasing concentration of  $[\text{Tb}_2(\text{DPQ})_2(\text{TFA})_6]$  (**3**) with  $\Delta\lambda=15$  nm (**a**) and  $\Delta\lambda=60$  nm (**b**) in 5mM Tris-HCl/5mM NaCl buffer (pH = 7.2) at 298 K. Arrow shows the quenching in the emission of BSA with addition of complex. Slit width (Excitation and Emission) = 5 nm.

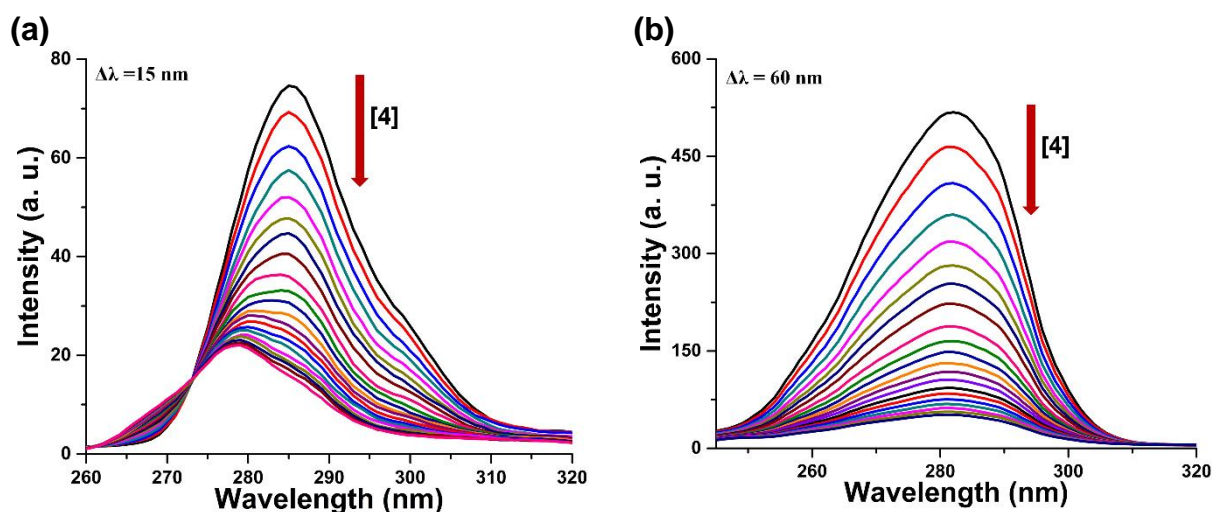


**Figure S15:** Synchronous emission spectra measurement of BSA ( $5 \mu\text{M}$ ) with increasing concentration of  $[\text{Tb}_2(\text{DPPZ})_2(\text{TFA})_6]$  (**4**) with  $\Delta\lambda=15$  nm (**a**) and  $\Delta\lambda=60$  nm (**b**) in 5mM Tris-HCl/5mM NaCl buffer (pH = 7.2) at 298 K. Arrow shows the quenching in the emission of BSA with addition of complex. Slit width (Excitation and Emission) = 5nm.

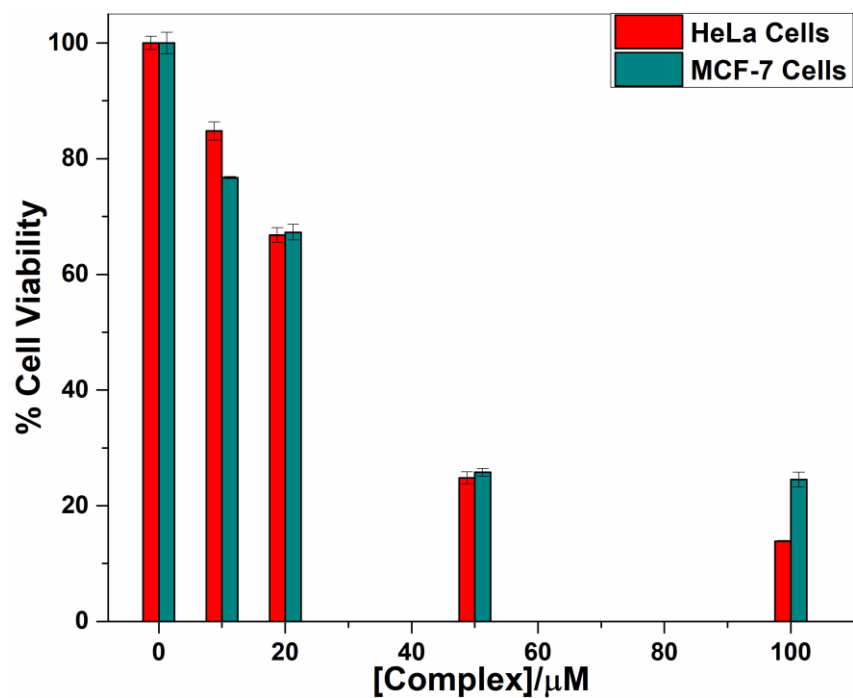


**Figure S16:** Cytotoxicity profile of  $[\text{Eu}_2(\text{DPQ})_2(\text{TFA})_6]$  (**1**) in HeLa and MCF-7 cell lines after 24 h incubation in at 37 °C measured using MTT assay.

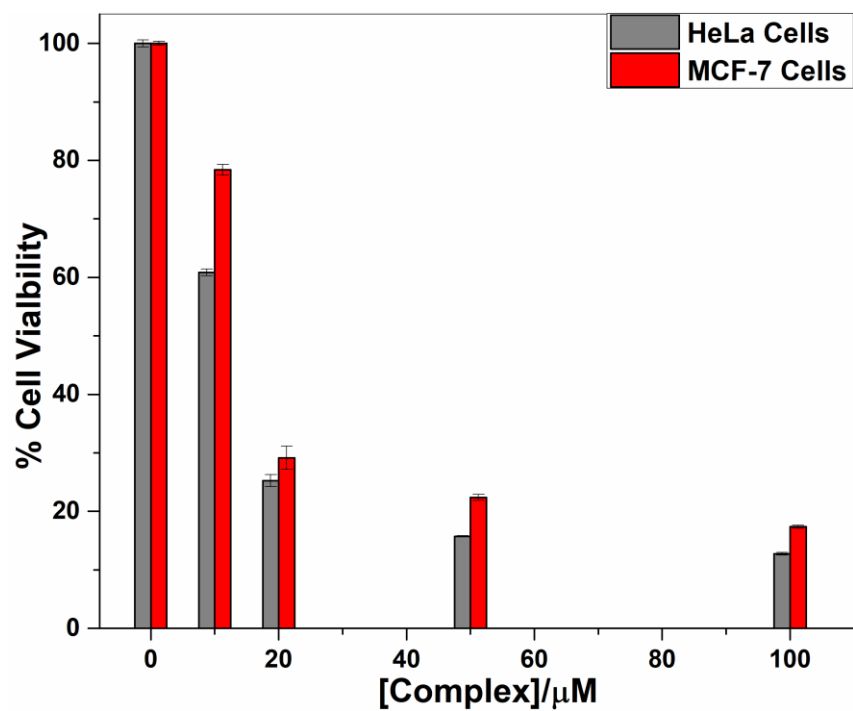


**Figure S17:** Cytotoxicity profile of  $[\text{Eu}_2(\text{DPPZ})_2(\text{TFA})_6]$  (**2**) in HeLa and MCF-7 cell lines after 24 h incubation at 37 °C measured using MTT assay.

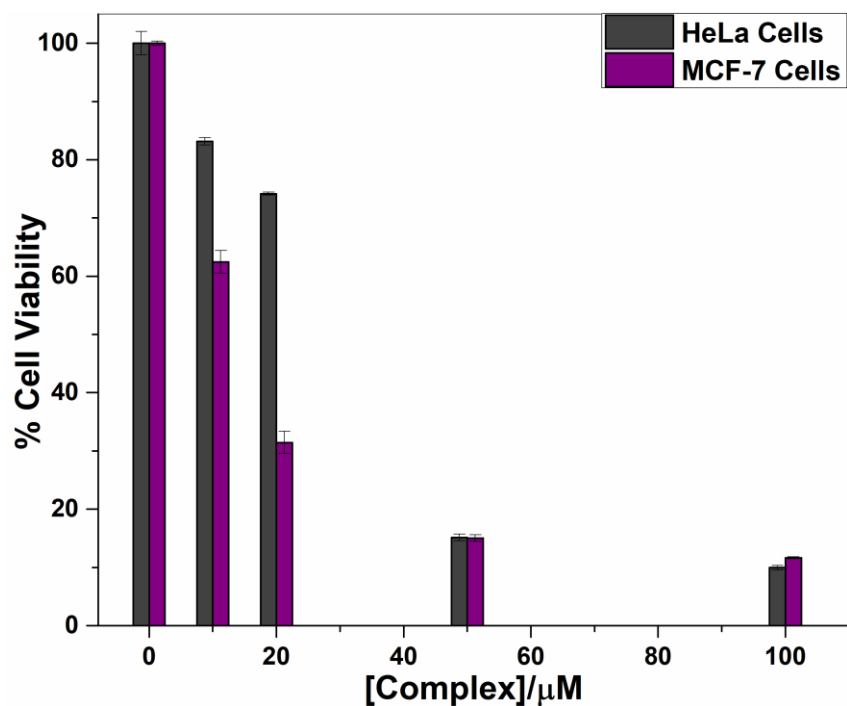


**Figure S18:** Cytotoxicity profile of  $[\text{Tb}_2(\text{DPQ})_2(\text{TFA})_6]$  (**3**) in HeLa and MCF-7 cancer cell lines after 24 h incubation at 37 °C measured using MTT assay.

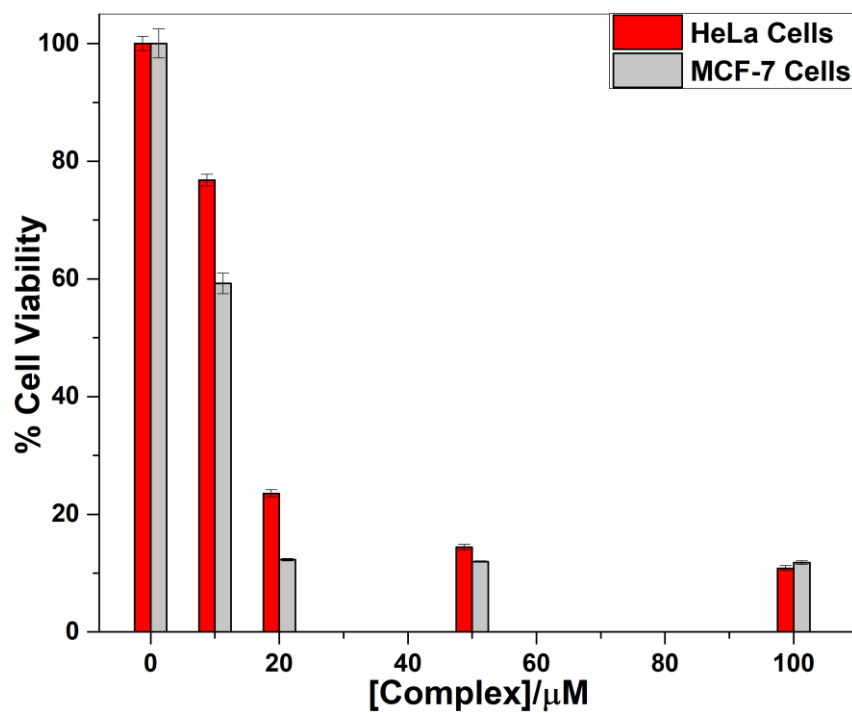


**Figure S19:** Cytotoxicity profile of  $[\text{Tb}_2(\text{DPPZ})_2(\text{TFA})_6]$  (**4**) in HeLa and MCF-7 cancer cell lines after 24 h incubation at 37 °C measured using MTT assay.

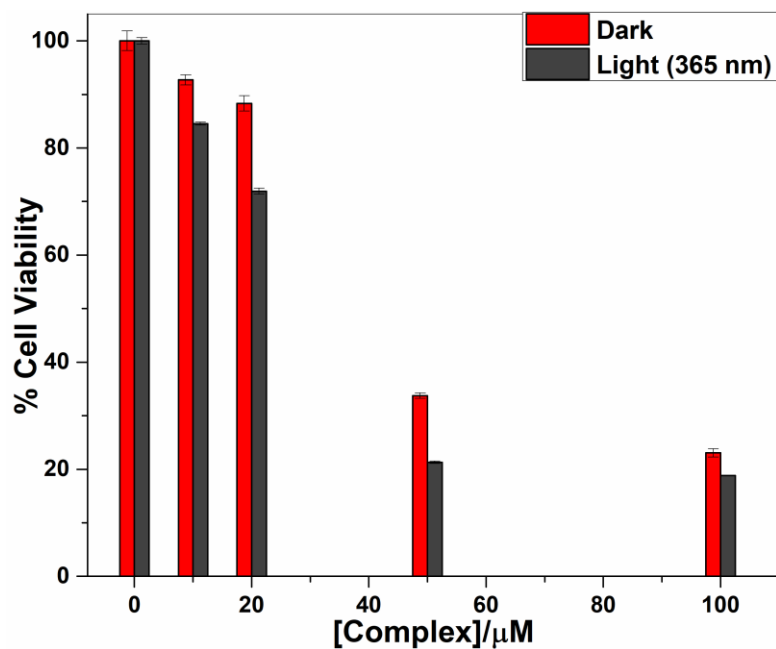


**Figure S20:** Photoinduced cytotoxicity profile of  $[\text{Eu}_2(\text{DPQ})_2(\text{TFA})_6]$  (**1**) in MCF-7 cell lines after 4 h incubation in dark at 37 °C followed by exposure to UV-A light (365 nm) for 1 h assessed using MTT assay.

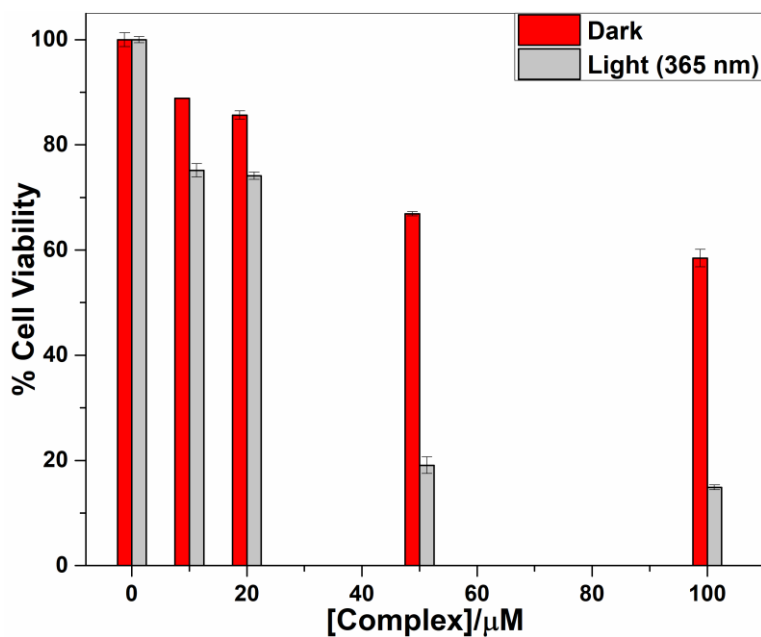


**Figure S21:** Photoinduced cytotoxicity profile of  $[\text{Tb}_2(\text{DPQ})_2(\text{TFA})_6]$  (**3**) in MCF-7 cell lines after 4 h incubation in dark at 37 °C followed by exposure to UV-A light (365 nm) for 1 h assessed using MTT assay.

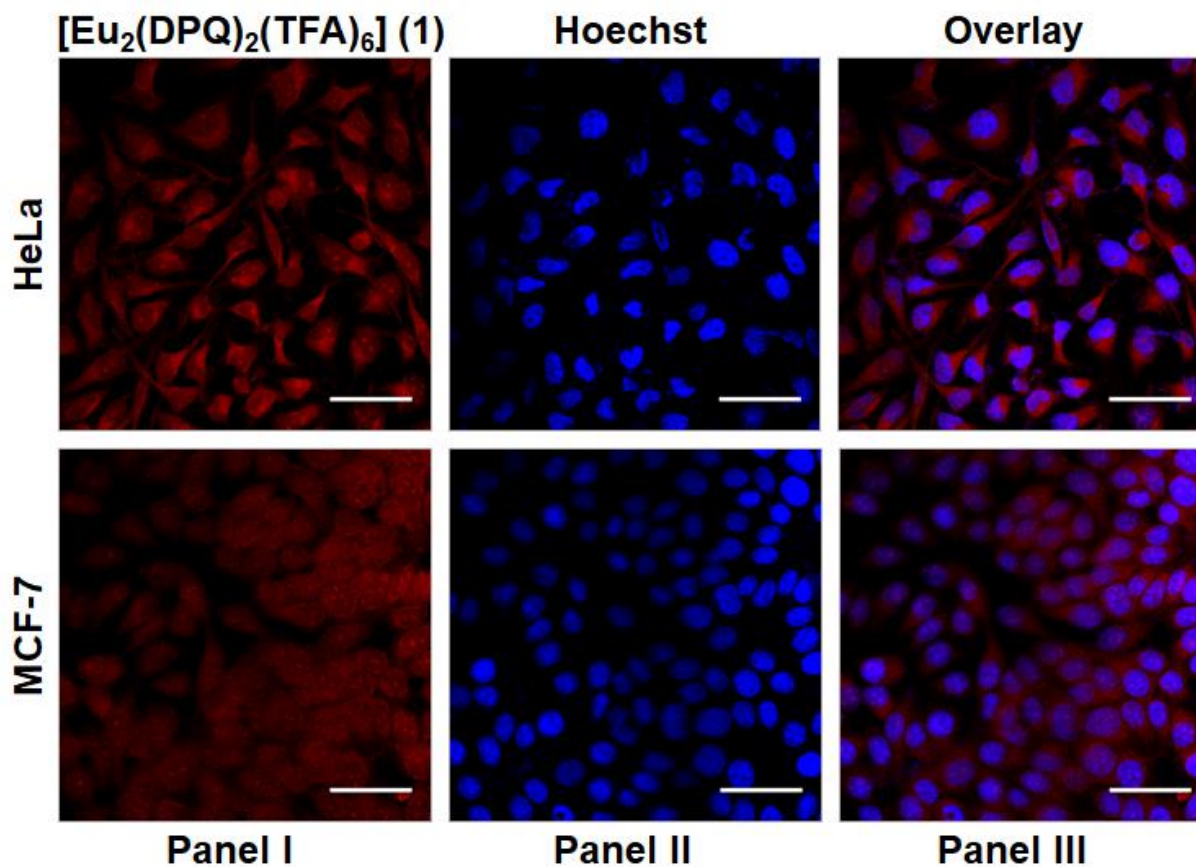


**Figure S22:** Confocal laser scanning microscopy images (CLSM) of cellular localization in the HeLa and MCF-7 cell lines treated with  $[\text{Eu}_2(\text{DPQ})_2(\text{TFA})_6]$  (**1**). **Panel I:** Cells incubated with complex **1** ( $10 \mu\text{M}$ ) for 4 h showing red emission at  $\lambda_{\text{ex}} = 405 \text{ nm}$ ; **Panel II:** Cells stained with nucleus staining dye Hoechst 33342 ( $5 \mu\text{g mL}^{-1}$ ) showing blue emission at  $\lambda_{\text{ex}} = 350 \text{ nm}$ ; **Panel III:** Merged images demonstrating nucleus and cytosolic localization of complex **1**. Scale bar =  $50 \mu\text{m}$ .

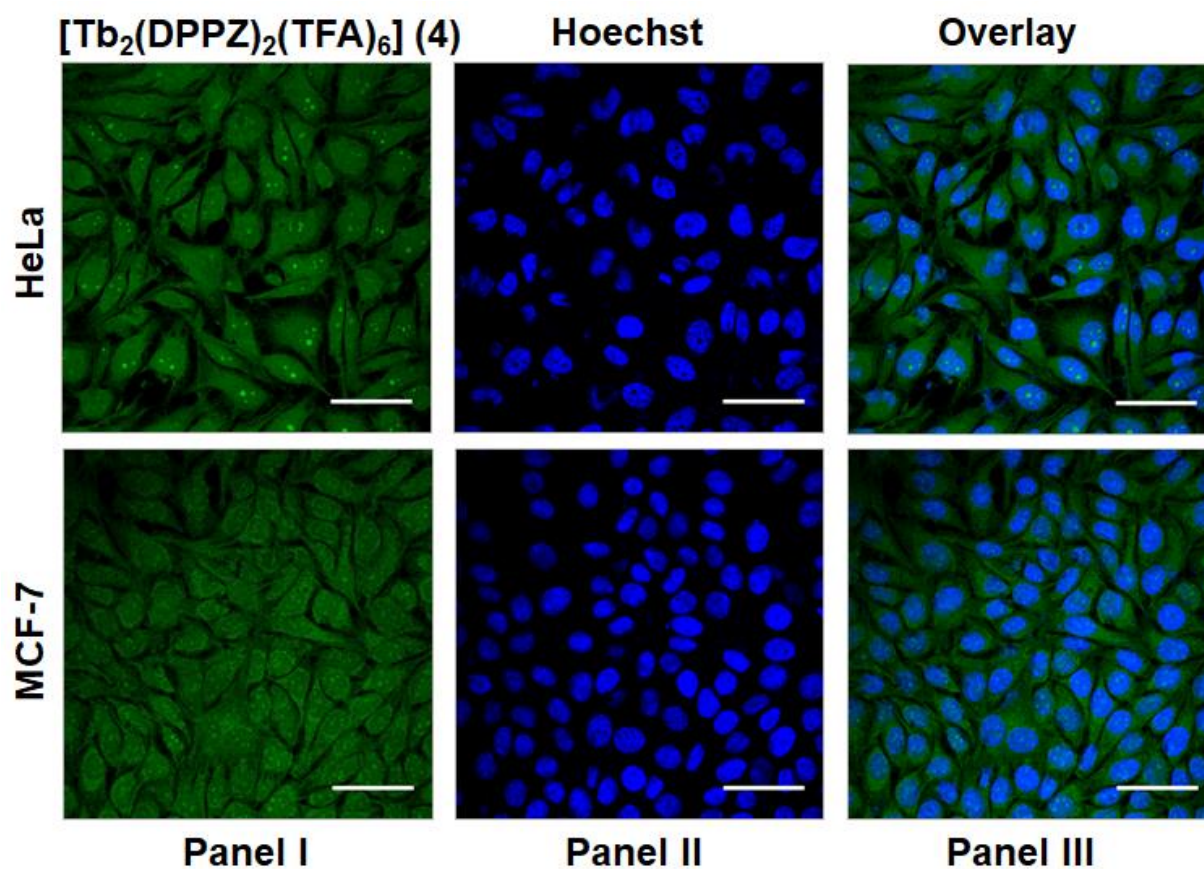


**Figure 23:** Confocal laser scanning microscopy images (CLSM) of cellular localization in the HeLa and MCF-7 cell lines treated with  $[\text{Tb}_2(\text{DPPZ})_2(\text{TFA})_6]$  (**4**). **Panel I:** Cells incubated with complex **4** ( $10 \mu\text{M}$ ) for 4 h showing green emission at  $\lambda_{\text{ex}} = 488 \text{ nm}$ ; **Panel II:** Cells incubated with nucleus staining dye Hoechst 33342 ( $5 \mu\text{g mL}^{-1}$ ) showing blue emission at  $\lambda_{\text{ex}} = 350 \text{ nm}$ ; **Panel III:** Merged images showing nucleus and cytosolic localization of complex **4**. Scale bar =  $50 \mu\text{m}$ .

## Experimental Section

### Materials and methods:

All the chemicals used in the synthesis were procured from either Sigma Aldrich or Alfa Aesar. Solvents were of spectroscopic grade or purified by standard literature procedures.<sup>1</sup> DPQ and DPPZ Ligands were prepared by treating phenanthroline 5, 6-dione, and ethylene diamine or 1, 2 diamino benzene.<sup>2</sup> The Hoechst 33342 dye for the nucleus staining was purchased from Thermo Fischer scientific. Trypsin- ethylenediaminetetraacetic acid (trypsin-EDTA), Dulbecco's modified eagle's medium (DMEM) and 3-(4,5-dimethylthiazol-2-yl)-2,5-diphenyltetrazolium bromide (MTT) were all procured from Sigma-Aldrich. Penicillin-streptomycin antibiotic solution (100X) was procured from Himedia. Dimethyl sulfoxide (DMSO), formaldehyde was obtained from Merck Chemicals, India. Fetal bovine serum (FBS) was purchased from Gibco Life Technologies. Human cervical carcinoma (HeLa) cells were procured from National Centre for Cell Science (NCCS), Pune. Human breast carcinoma (MCF-7) cells were procured as a kind gift from Prof. Bushra Ateeq, Indian Institute of Technology Kanpur, India.

A Perkin Elmer model 1320 FT-IR spectrometer used to record the FT-IR spectra in the range 4000-400  $\text{cm}^{-1}$  using KBr pellets. UV-Vis electronic absorption behavior of the ligand and complexes were studied on Varian V670 spectrometer at 298 K. Emission spectral measurement of the ligands and time-resolved luminescence spectra of the complexes were recorded on an Agilent Cary Eclipse fluorescence spectrophotometer. Luminescence decay measurement of the  $\text{Eu}^{\text{III}}$  at 615 nm and  $\text{Tb}^{\text{III}}$  at 545 nm in the complexes at  $\lambda_{\text{ex}} = 290$  nm excitation wavelength. The number of the water molecules in the first coordination sphere of the respective  $\text{Eu}^{\text{III}}$  and  $\text{Tb}^{\text{III}}$  complexes was calculated from the modified Horrock's equation using their decay lifetime in  $\text{H}_2\text{O}$  and  $\text{D}_2\text{O}$ .<sup>3</sup> The overall quantum yield ( $\phi_{\text{overall}}$ ) of the luminescence of the complexes **1-4** were calculated from the following equation taking quinine sulphate as reference standard.<sup>4</sup>

$$\phi_{\text{overall}} = \phi_{\text{ref}} A_{\text{ref}} I n^2 / A I_{\text{ref}} n_{\text{ref}}^2$$

Where A is the absorbance at the excitation wavelength, I represent the area under the emission plot, n is the refractive index of the respective solvent and  $\phi_{\text{ref}}$  is the quantum yield of the quinine sulphate as a reference at RT.

## References:

1. D. D. Perrin, W. L. F. Armarego and D. R. Perrin, *Purification of Laboratory Chemicals*, Pergamon Press, Oxford, **1980**.
2. (a) J. E. Dickeson and L. A. Summers, *Aust. J. Chem.*, 1970, **23**, 1023 -1027; (b) J. G. Collins, A. D. Sleeman, J. R. Aldrich-Wright, I. Greguric and T. W. Hambley, *Inorg. Chem.*, 1998, **37**, 3133 -3141.
3. (a) W. D. Horrocks Jr. and D. R. Sudnick, *J. Am. Chem. Soc.*, 1979, **101**, 334 -340; (b) A. Beeby, I. M. Clarkson, R. S. Dickins, S. Faulkner, D. Parker, L. Royle, A. S. de Sousa, J. A. G. Williams and M. Woods, *J. Chem. Soc., Perkin Trans. 2*, 1999, 493 -504.
4. J. R. Lakowicz, *Principles of Fluorescence Spectroscopy*, Springer, New York, **2006**.